Journal of Information Systems Engineering and Management
2025, 10(53s)
e-ISSN: 2468-4376
https://www.jisem-journal.com/

Research Article

Design and Testing of a Novel MIMO Antenna for the 28 GHz Millimetre Wave Band

Malini Soman[1*], Pardeep Kumar[2], Manish Sharma[3]
[1*]*Department of Electronics & Communication SGT University Gurugram, Haryana, India* malini_feat@sgtuniversity.org
[2]*Department of Electronics & Communication Engineering SGT University Gurugram, Haryana, India*
pardeep.lamba@gmail.com
[3]*SMIEEE Chitkara University Institute of Engineering and Technology Chitkara University, Punjab, India*
manish.sharma@chitkara.edu.in

ARTICLE INFO

Received: 29 Dec 2024

Revised: 15 Feb 2025

Accepted: 24 Feb 2025

ABSTRACT

This study focuses on designing and assessing a novel 5G-specific Multiple Input Multiple Output antenna (MIMO) functioning inside the millimeter wave band at 28 GHz. Two radiating components dominate the antenna. The system has two components: the primary patch and a parasite element. The primary patch is energized via a micro-strip line that has an inset feed, while the parasite element is energized by capacitive coupling. Optimal matching of impedance at 28 GHz is attained by refining the design parameters of the proposed antenna via extensive parametric analysis. The research investigates an operational frequency of surface current distributions. A 4-port effective MIMO system is established using the developed antenna. An analysis of the MIMO system's performances for ECC, DG, and CCL indicates its efficacy. Experimental assessments of the single-element antennas and the MIMO show outstanding matching of impedance throughout the frequency ranges, supported by the modeling results. The antenna has a gain of 7.8 dBi at 28 dBi.

Keywords: MIMO, Antenna, ECC, DG, CCL

1. INTRODUCTION

In the modern world, wireless communication is having an impact on a wide variety of domains, (example such as dependable and efficient remote communication; remotely automated and robot-controlled machines; machine-to-machine communication; the Internet of Things (IoT); unmanned transportation systems; smart grid concepts in power transmission and distribution; digital banking systems; and smart home HDTV through effective satellite communication systems). These technologies are providing a significant contribution to the enhancement of human lives (Costanzo, et al., 2016; Kiani, et al., 2022; Kiani, et al., 2022). With the fast development of wireless communication technologies over the last several decades, antenna engineers have been striving to develop innovative and efficient solutions for continuous and uninterrupted connection with flawless and consistent reception of the signals. This is in response to the fact that the growth of wireless communication technologies has occurred very rapidly (Ibrahim, 2019). Due to the fast increase in mobile data and the widespread use of smartphones, wireless service providers often confront issues that have never been seen before when they seek to solve a worldwide bandwidth obstruction (Munir, et al., 2023).

MIMO systems represent a notable technological innovation capable of enhancing channel capacity and communication dependability while functioning within limited bandwidth and power requirements. Alongside the 4G standards and Wi-Fi, they were also included into several additional communication technologies. MIMO systems will remain pertinent within the context of the 5G specification (Hong, 2017). The MIMO system will provide the ideal combination of bandwidth and channel capacity in the 5G sub-28GHz frequencies. In the millimeter-wave the spectrum, where the exact location of the device that communicates is uncertain, MIMO will enhance channel bandwidth in a multi-path scenario, with both transmitters and receivers in close proximity to each other (Hussain, et al., 2022). [Figure 1] delineates the classification of various MIMO antenna designs.

Journal of Information Systems Engineering and Management
2025, 10(53s)
e-ISSN: 2468-4376
https://www.jisem-journal.com/

Research Article

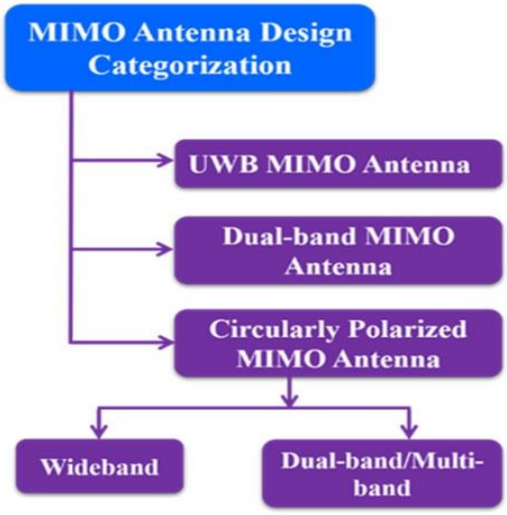

Figure 1: Classification of MIMO antenna

A MIMO system consists of numerous essential parts, including the antenna. The antenna's design significantly impacts the whole system's overall performance. The optimal scenario would include an antenna exhibiting exceptional port isolation among its components, while simultaneously ensuring that the distributions of radiation of these elements are configured to maintain the independence of the MIMO channels. The Envelope correlated coefficient (ECC) is an evaluation metric for MIMO antennas that quantifies the degree of correlation created across channels due to the antenna design. This MIMO antenna is designed to exhibit reduced ECC values and effective port isolation among its antenna elements (Sharawi, 2013). [Table 1] indicates that investigators have created multiple antennas functioning at wavelengths of 28 GHz and 38 GHz.

Table 1: Comparison of previous work on several antenna operate at frequencies of 28 and 38 GHz.

Authors (Year) [Reference]	Aim of the Study	No. of Ports	Gain (dBi)	ECC	CCL (bits/s/Hz)	DG (dB)
Tiwari, et al. (2024) (Tiwari, et al., 2024)	A 5G millimeter wave 28/38 GHz wearable antenna with a 4×4 MIMO design that is both flexible and durable.	4	7.73	<0.03	<0.15	9.87
Elabd and Al-Gburi (2024) (Elabd & Al-Gburi, 2024)	5G Cellular Devices' Ultra-Compact 28/38 GHz 4-Port MIMO Antenna with a Metamaterial-Inspired EBG Structure and SAR Analysis.	4	8.9	$<3\times 10^{-5}$	<0.03	10
Gupta, et al. (2024) (Gupta, et al., 2024)	The n261 band is being studied for body-centric communication using a 27 GHz 8-port MIMO antenna.	8	4.64	<0.005	NR	9.97
Munir, et al. (2024) (Munir, et al., 2024)	The mm-Wave and 5G futures are addressed by a 4-port tri-circular ring MIMO antenna.	4	6.6	<0.001	<0.16	9.9
Nasri, et al. (2024)	An innovative 4 port wideband (21.8-29.1 GHz) MIMO antenna	4	5.76	<0.004	<0.4	9.995

Journal of Information Systems Engineering and Management
2025, 10(53s)
e-ISSN: 2468-4376
https://www.jisem-journal.com/

Research Article

(Nasri, et al., 2024)	designed for 5G NR networks, formed like an arc.					
Aboualalaa and Mansour (2023) (Aboualalaa & Mansour, 2023)	A 5G millimeter-wave antenna array with a split-ring structure and dual-band end-fire 4-element MIMO.	4	7.9	$<10^4$	NR	10
Ahmad, et al. (2022) (Ahmad, et al., 2022)	A tiny 2-element MIMO antenna designed for 5G networks.	2	6	<0.001	NR	>9.8
Farahat and Hussein (2022) (Farahat & Hussein, 2022)	MIMO antenna with dual bands (28 and 38 GHz) designed for use in 5G mobile applications.	2	6.6	Value not given	NR	Value not given
Tsao, et al. (2022) (Tsao, et al., 2022)	Dual-polarization, dual-band CPW Fed MIMO antenna for 5G mobile communications at 28 and 38 GHz.	2	8	0.0001	<0.1	10
Khan, et al. (2022) (Khan, et al., 2022)	A Compact mm-Wave MIMO Array for Future Wireless Networks.	4	5.66	0.008	NR	>9.95

This paper presents a comprehensive study on the development of a MIMO antenna specifically designed for operation in the 28 GHz mm-wave band. The 28 GHz frequency is a key component of the millimeter-wave spectrum, which is recognized for its potential to suggestively improve data rates and capacity in 5G and beyond wireless systems. The proposed composite microstrip patch antenna for 5G mobile devices is a lightweight, small, and single-element design that operates in the 28 GHz mm-wave bands. To build a 4-Ant MIMO antenna system, the suggested single-element antenna is used. The adjoining components of the suggested antenna have very weak coupling coefficients, making it suitable for use in small antenna arrays for beam shaping and direction of arrival detection. Fabrication of the planned composite antenna is carried out to experimentally validate the findings of the simulation.

By leveraging advanced design techniques and innovative fabrication methods, the proposed MIMO antenna aims to provide radiation patterns, high peak gain, increased radiation efficiency, negligible ECC, acceptable Total Active Reflection Coefficient (TARC), Minimal Channel Capacity Losses (CCL), and low Mean Effective Gain (MEG) at 28 GHz. The study includes a detailed analysis of the antenna's design parameters, simulation results, and experimental validation. It offers valuable insights into its practical implementation and potential applications in high-frequency communication systems.

2. ADVANTAGES OF MIMO SYSTEM

Gigabit data speeds are in increasing demand due to the expanding variety of mobile apps, which need to accommodate users with varying degrees of mobility. Modern mobile devices are including MIMO antennas to meet this need. Improved spectrum efficiency, higher data rates, more capacity, and continuous signaling are just a few of the ways that mobile devices can enhance the quality of service using MIMO technology. The following are a few of the benefits:

Journal of Information Systems Engineering and Management
2025, 10(53s)
e-ISSN: 2468-4376
https://www.jisem-journal.com/

Research Article

2.1 Increased Data Rates

MIMO technology enables faster data rates than conventional SISO systems by allowing the transmission of several data streams across a single frequency band. The total system throughput grows in direct proportion to the MIMO layer number [19].

2.2 Improved Signal Quality

MIMO technology is useful for enhancing signal quality by mitigating interference, noise, and fading. Figure 2 shows the properties of interference and fading at the coverage boundary caused by the large beamwidth of base station antennas in conventional Single Input Single Output (SISO) systems. In contrast, [Figure 3] shows the results of improved coverage and reduced interference at the coverage boundary caused by MIMO at g-NodeB (5G base station antennas) (Raj, et al., 2023).

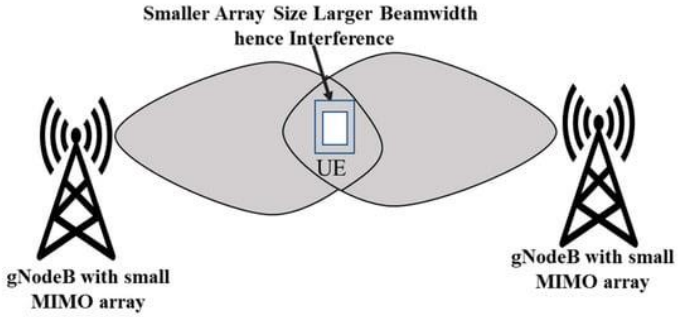

Figure 2: Coverage border interference increases with smaller array size and larger beamwidth (Raj, et al., 2023).

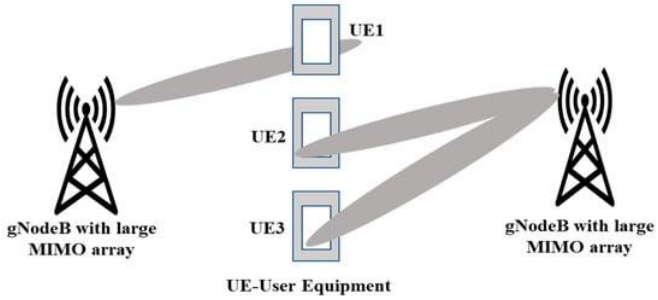

Figure 3: Larger array size sharper beam low interference (Raj, et al., 2023).

2.3 Increased Range and Coverage

MIMO antenna can increase the coverage area and bandwidth of wireless networks by enhancing connection quality and decreasing the probability of signal dropouts. Compared to a traditional SISO system, a bigger MIMO array or massive MIMO could improve coverage area by generating a more directed beam [Figure 4] (Raj, et al., 2023).

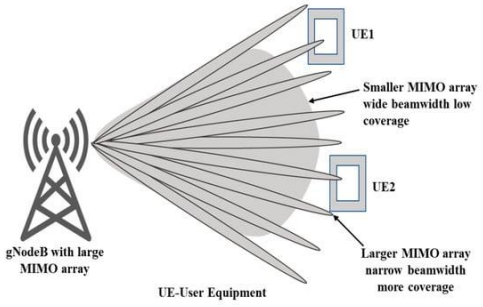

Figure 4: Directional beams cover more and offer a better signal-to-noise ratio.

Journal of Information Systems Engineering and Management
2025, 10(53s)
e-ISSN: 2468-4376
https://www.jisem-journal.com/

Research Article

3. SINGLE ELEMENT ANTENNA DESIGN

Figure 5a-d serves as a visual illustration of the stages of antenna design. As shown in Figure 5a, the first stage consideration was made for an octagonal-shaped radiator, which was supplied by a microstrip line with a resistance of 50 Ω. With its high eccentricity, the radiator was able to accommodate numerous modes, which is a need for the radiator. The surface that was not grounded and was located under the antenna radiating patch operated as a resistance that was not balanced. A tiny slit in the shape of a U was cut out of the ground surface to provide the necessary impedance matching between the patch and the feed line in stage 2, as shown in [Figure 5b]. An HSRR was implanted in the antenna radiator, as shown in Figure 5c, to eliminate the 5.5 GHz (WLAN) band that was causing interference (stage 3). During the next stage, which is seen in Figure 5d, an extra HSRR (which was contrasted with the HSRR that was used in stage-3) was placed onto the radiator to get rid of the 3.5 GHz (Wi-MAX) band signals that were causing interference (stage-4) (Patre & Singh, 2016).

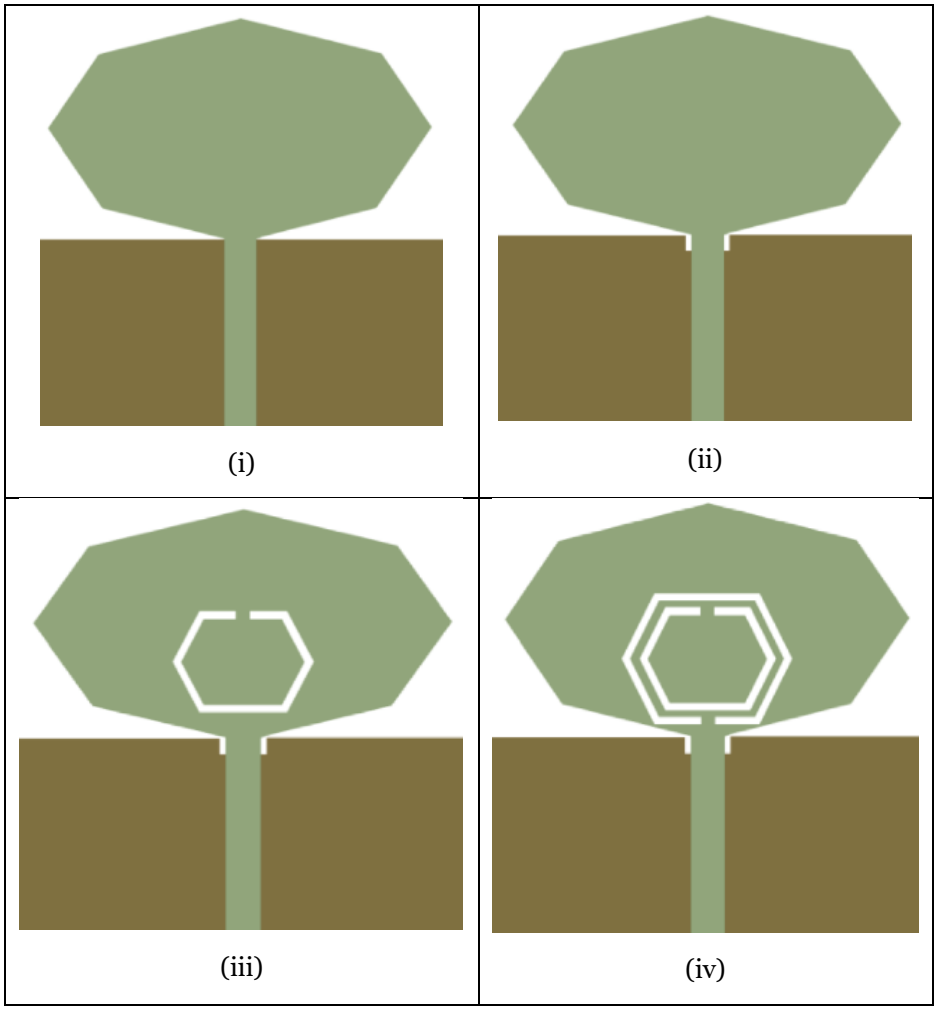

Figure 5: The design steps for an octagonal monopole antenna: (**i**) stage-1; (**ii**) stage-2; (**iii**) stage-3; (**iv**) stage-4.

The given single-element antenna design is shown schematically in [Figure 6]. The single-element antenna contains of a rectangular ground plane and an octagonal resonating element that is supplied by microstrip lines. An antenna with an HSRR implanted in its octagonal patch could notch frequencies in the Wi-MAX (5.2 GHz) and WLAN (7.3 GHz) bands. A superior impedance match could be achieved by cutting a U-shaped loop into the monopole antenna's ground plane. The FR-4 dielectric material has a relative permittivity of 5.5 and is 0.9 mm thick; it is imprinted with the antenna. With the help of an ANSYS HFSS tool, the developed antenna is simulated, designed, and put into function. The data on the octagonal monopole element's dimensions can be found in [Table 2].

Journal of Information Systems Engineering and Management
2025, 10(53s)
e-ISSN: 2468-4376
https://www.jisem-journal.com/

Research Article

Table 2: Size optimization for the suggested antenna.

Parameter	Dimension (mm)	Parameter	Dimension (mm)
L	27	W1	2.6
W	20	S4	1.2
a	6.2	W2	3.1
b	9	W3	0.7
f	12.04	W4	1.6
S1	6	W5	1.6
S2	5.4	L1	63
S3	5	W6	0.8

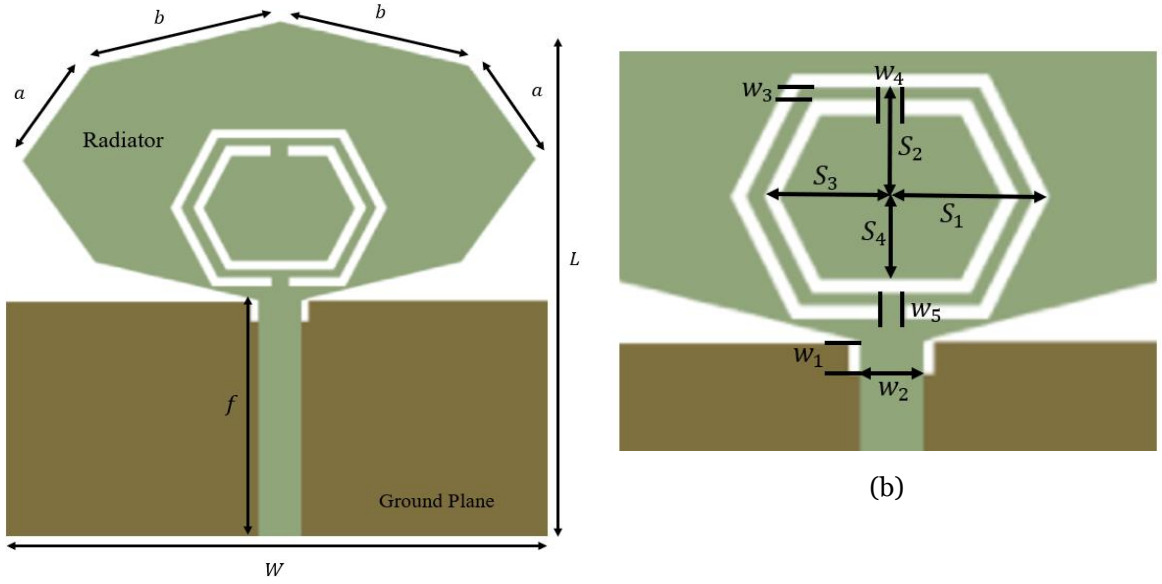

Figure 6: A schematic of the suggested octagonal-shaped monopole antenna: (a) schematic design; (b) inflamed view of the HSRR

4. PROPOSED MIMO ANTENNA DESIGN

For efficient MIMO operation, a compact four-ant MIMO antenna system design with dimensions of $51mm \times 51mm \times 0.9mm^3$ has been developed; this arrangement is compact. [Figure 7] represents the configuration of the system, which is included of 4 dual-band antennas. The horizontal direction is received by two of the antennas, while the vertical direction is also received by the other two antennas. To reduce the amount of current that flows back and forth between the antennas, a square gap is placed in the middle of the MIMO antenna configuration. This makes it possible to strengthen the MIMO performance at high data rates while simultaneously lowering the coupling between the antenna parts. To ensure that the suggested antenna design, dimension optimization, and simulations were carried out successfully, *Ansoft HFSS were* used. Among the MIMO parameters that are investigated are the coupling coefficients, the ECC, the DG, and the radiation patterns. Their performance is

Journal of Information Systems Engineering and Management
2025, 10(53s)
e-ISSN: 2468-4376
https://www.jisem-journal.com/

Research Article

characterized by these characteristics. Two vertical and two horizontal antennas allow this MIMO system design to receive and transmit orthogonal polarizations, making it ideal for polarization diversity schemes. Additionally, it is suitable for spatial diversity schemes since the four antennas have four distinct spatial positions. As seen in [Figure 8], the prototype is the product of fabrication on the polyester substrate.

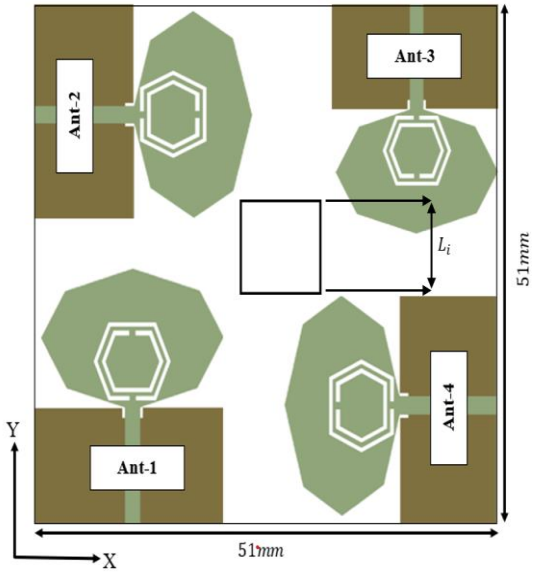

Figure 7: Suggested 4-Ant dual-band MIMO antenna system shape

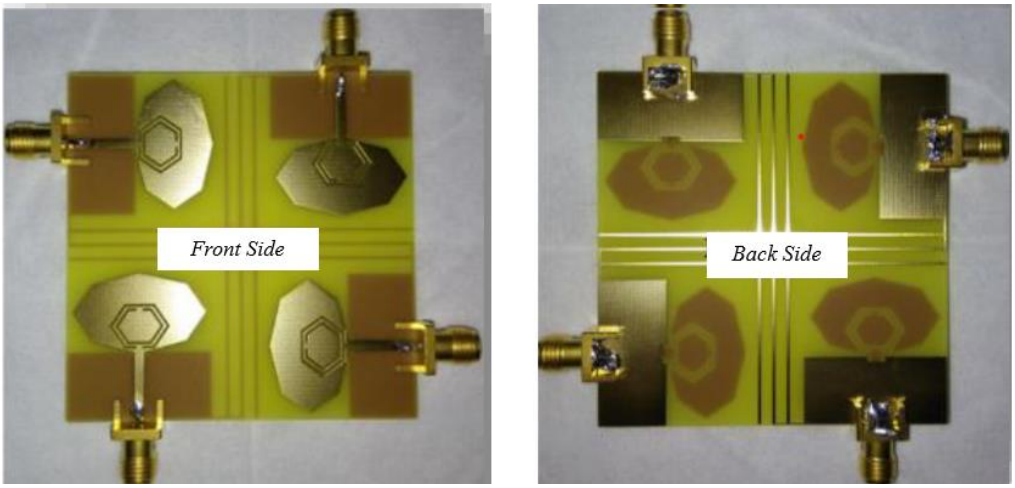

(a) (b)

Figure 8: Fabricated MIMO antenna: (a) front side and (b) backside

5. MIMO ANTENNA DESIGN APPROACHES

Modern wireless communication systems have greatly emphasized MIMO antennas because they boost range and performance by using several pathways to send and receive data (Niu, et al., 2019). It should be mentioned that for the MIMO antenna elements to operate independently and send or receive signals at the same time without degrading the antenna characteristics, there must be substantially isolated components within the same MIMO system.

Some diversity parameters are used to guarantee the quality of a MIMO antenna, alongside S-parameters and radiation characteristics. Before using MIMO antennas in a real-world application, make sure they meet the diversity parameters' specified values. This section therefore briefly discusses some fundamental diversity parameters for MIMO antennas.

Journal of Information Systems Engineering and Management
2025, 10(53s)
e-ISSN: 2468-4376
https://www.jisem-journal.com/

Research Article

5.1 Envelope Correlation Coefficient (ECC)

The ECC is a diversity metric that shows how well neighboring components of a MIMO antenna are correlated with one another. Radiation patterns or S-parameters can be used to determine it (Raj, et al., 2021). The ECC explains how diverse radiating components in MIMO systems have distinct radiation patterns, hence it's preferable to utilize that value when evaluating the far-field radiation pattern. Equation (1) provides the formula for ECC through the use of radiation pattern data from MIMO architecture (Tiwari, et al., 2022):

$$ECC_{qp} = \frac{|\int_0^{2\pi}\int_0^{\pi}(E^*_{\theta p}E^*_{\theta q}P_\theta XPR + E^*_{\varphi p}E_{\varphi p}P_\varphi)d\Omega|^2}{\alpha \times \beta} \quad (1)$$

$$\alpha = \int_0^{2\pi}\int_0^{\pi}(E^*_{\theta q}E^*_{\theta q}P_\theta XPR + E^*_{\varphi q}E_{\varphi q}P_\varphi)\, d\Omega \quad (2)$$

$$\beta = \int_0^{2\pi}\int_0^{\pi}(E^*_{\theta p}E^*_{\theta p}P_\theta XPR + E^*_{\varphi p}E_{\varphi p}P_\varphi)\, d\Omega \quad (3)$$

where XPR is the cross-polarization level, which is the ratio of average power along the phi and theta directions. In a practical environment, the acceptable limit of ECC must be <0.5.

5.2 Diversity Gain (DG)

DG is a measure of a MIMO antenna's performance and reliability in a wireless system. Hence, the MIMO antenna's DG has to be sufficiently high, about 10 dB, to remain inside the applicable frequency range. Equation (4) can be used to calculate the DG by using the ECC value (Garg & Jain, 2020):

$$DG = 10 \times \sqrt{1 - |ECC_{qp}|^2} \quad (4)$$

5.3 Channel Capacity Loss (CCL)

A communication channel's capacity to carry data with almost no loss is known as its channel capacity limit, or CCL. The default CCL value is lower than 0.4 bits/s/Hz for any particular MIMO.

Equation (5) gives the CCL expression using S-parameters (Chae, et al., 2007; Khalid, et al., 2020):

$$CCL = -\log_2 \det(\vartheta^\mu) \quad (5)$$

Where

$$\vartheta^\mu = \begin{bmatrix} \xi_{11} & \xi_{12} \\ \xi_{21} & \xi_{22} \end{bmatrix} \quad (6)$$

and

$$\begin{aligned} \xi_{11} &= 1 - [|S_{11}|^2 + |S_{12}|^2] \\ \xi_{12} &= -[S^*_{11}S_{12}S^*_{21}S_{12}] \\ \xi_{21} &= -[S^*_{22}S_{21}S^*_{12}S_{21}] \\ \xi_{22} &= 1 - [|S_{22}|^2 + |S_{21}|^2] \end{aligned} \quad (7)$$

5.4 Mean Effective Gain (MEG)

MEG of the MIMO antenna is another important characteristic for diversity applications. MEG is defined as the average amount of power that is established by a system when it is operating in a fading environment (Zahra, et al., 2021). It is possible to determine the value of MEG by using the following equation (8) (Hussain, et al., 2020):

$$MEG = 0.5 \times \mu_{tr} = 0.5 \times \left[1 - \sum_{j=1}^{l}(|S_{ij}|)\right] \quad (8)$$

6. HFSS SOFTWARE SPECIFICATION

HFSS is an industrial finite-element solver for magnetic structures created by Ansys. It is among the several commercial tools used for antenna design and the development of advanced RF electrical circuit components, including filters, lines for transmission, and packaging. Researcher Zoltan was Cendes and his students at Carnegie

Journal of Information Systems Engineering and Management
2025, 10(53s)
e-ISSN: 2468-4376
https://www.jisem-journal.com/

Research Article

Mellon University in New York originated the concept. Ansoft was founded by Professor Cendes and his elder brother Nicholas Cendes, who also provided HFSS packaging. It is a high-performance full-wave electromagnetic field simulator that models passive devices in 3D and makes use of a graphical user interface that is familiar to users of Microsoft Windows (Sridevi & Mahendran, 2017).

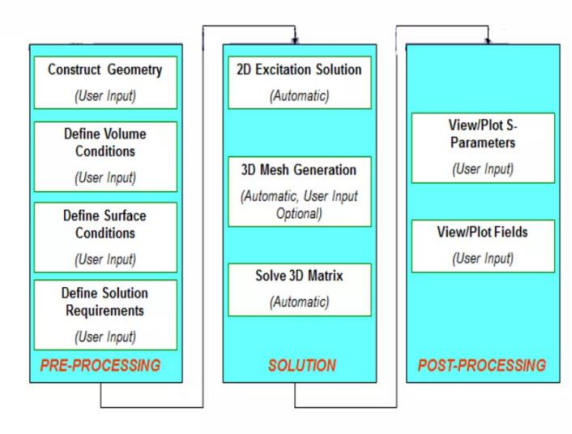

Figure 9: HFSS analysis design flow chart (Sridevi & Mahendran, 2017).

7. RESULTS AND DISCUSSIONS

Here, they study the evaluation of the single-element antenna and the suggested MIMO antenna system using microwave electromagnetic calculations and experimental measurements.

7.1 Gain (dBi)

The [figure 10] illustrates the relationship between Gain (in dBi) and Frequency (in GHz). The x-axis represents the gain in dBi, and the y-axis shows the frequency range from 25 GHz to 31 GHz.

- At 25 GHz, the gain starts around 1 dBi. As the frequency increases, the gain rises sharply.
- The gain reaches its peak value of approximately 8 dBi around 28 GHz, indicating maximum performance at this frequency.
- Beyond 28 GHz, the gain begins to decline, gradually dropping to around 4 dBi by the time the frequency reaches 31 GHz.

The plot indicates that the system achieves the highest gain near 28 GHz, where performance is optimal, while at lower and higher frequencies (25 GHz and 31 GHz), the gain decreases significantly, implying reduced performance.

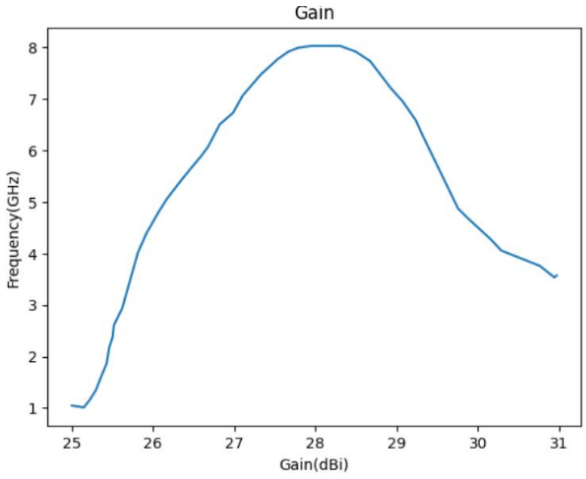

Figure 10: Simulation and measurement of suggested antenna gain

Journal of Information Systems Engineering and Management
2025, 10(53s)
e-ISSN: 2468-4376
https://www.jisem-journal.com/

Research Article

7.2 Efficiency

The [figure 11] is a plot showing the efficiency of a system as a function of frequency. The x-axis represents the frequency (in an arbitrary unit), ranging from 25 to 31, while the y-axis denotes efficiency values, ranging from 1 to 8. The efficiency increases rapidly from a value of around 1 at 25 units of frequency, peaking at approximately 8 near 28 units of frequency. After this peak, the efficiency gradually decreases, dropping to about 3.5 at 31 units of frequency. This suggests that the system performs optimally around 28 units of frequency, with diminishing efficiency outside this range.

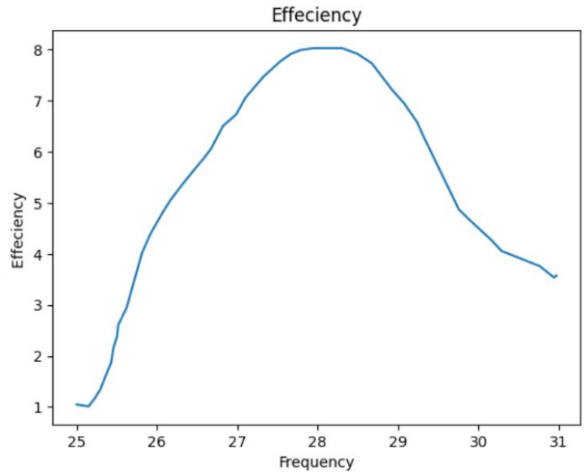

Figure 11: Simulation and measurement of suggested antenna efficiency

7.3 Radiation pattern

The [figure 12] demonstrates the radiation patterns of two materials: FR4-based (red) and PP-based (green). The radial axis represents the gain in decibels (dB), with values like 0, -5, -17.5, and -30 dB indicating the radiation efficiency at various angles (0° to 360°). The FR4-based material generally shows higher radiation efficiency, with peaks reaching closer to 0 dB around angles like 60° and 300°, while the PP-based material's peaks are slightly lower, near -5 dB. Both materials show similar behavior, with dips in radiation efficiency between -17.5 dB and -30 dB in several directions (e.g., near 180° and 240°). The FR4-based material has a broader, more pronounced radiation pattern compared to the PP-based material, indicating slightly better overall efficiency across multiple angles.

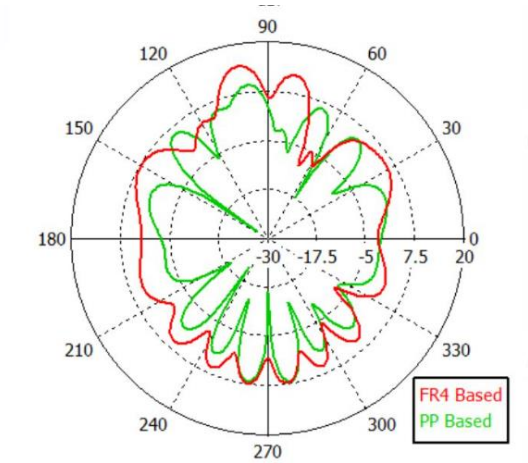

Figure 12: Simulation and measurement of suggested antenna radiation pattern

7.4 Envelope Correlation Coefficient (ECC)

The [figure 13] depicts the relationship between Frequency (in GHz) and ECC.

Journal of Information Systems Engineering and Management
2025, 10(53s)
e-ISSN: 2468-4376
https://www.jisem-journal.com/

Research Article

- At the lower frequency end (around 25 GHz to 26 GHz), the ECC fluctuates significantly, showing some sharp peaks and dips. The maximum ECC value here reaches close to 0.003.
- As the frequency increases beyond 26 GHz, the ECC drops sharply and stabilizes at values very close to zero.
- Between 27 GHz and 28 GHz, the ECC remains at a low value, close to 0.0005 or lower, indicating minimal correlation.
- After 28 GHz, the ECC begins to rise again, steadily increasing towards higher values as it approaches 30 GHz.

The simulated ECC in this range highlights that there is low correlation (close to zero) between the frequencies bands around 27-28 GHz, which suggests that these frequencies provide good isolation. However, frequencies outside this range, particularly near 25-26 GHz and around 30 GHz, exhibit higher ECC values, indicating more correlation and potentially reduced isolation.

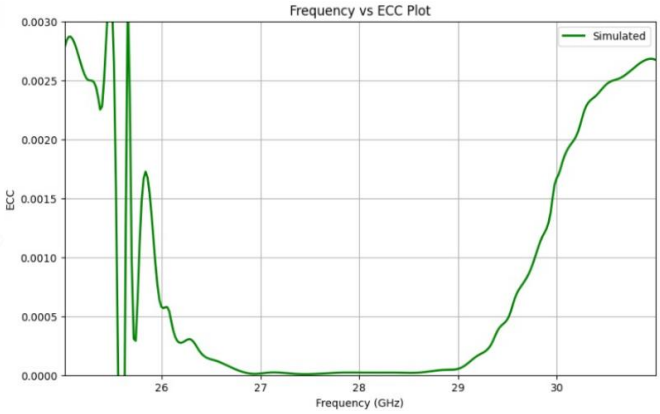

Figure 13: Simulation and measurement of suggested antenna ECC .

7.5 Diversity Gain (DG)

The [figure 14] illustrates the relationship between Frequency (in GHz) and DG (in dB).

- The diversity gain starts at around 9.988 dB at 25 GHz. As the frequency increases, the DG quickly rises and reaches a maximum value of 10 dB near 26 GHz.
- Between 26 GHz and 28 GHz, the DG remains nearly constant at the maximum value of 10 dB, indicating very high diversity gain in this frequency range.
- After 28 GHz, the DG slightly decreases, with the value dropping just below 10 dB near 31 GHz.

The flatness of the DG values close to 10 dB over the majority of the frequency range (from approximately 26 GHz to 30 GHz) suggests excellent diversity performance, indicating strong signal reception with minimal correlation between the signals in this frequency range. The minor dip after 30 GHz shows a slight reduction in performance, though the diversity gain still remains high.

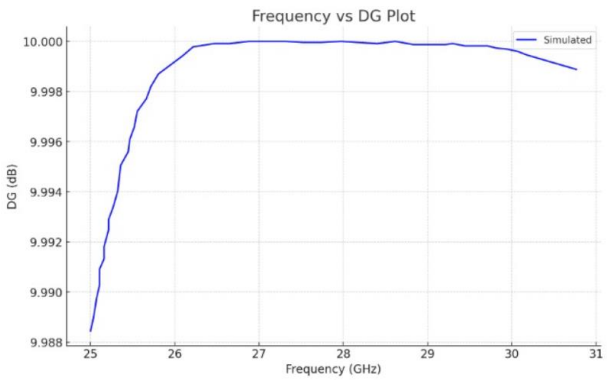

Figure 14: Simulation and measurement of suggested antenna DG

Journal of Information Systems Engineering and Management
2025, 10(53s)
e-ISSN: 2468-4376
https://www.jisem-journal.com/

Research Article

7.6 Mean Effective Gain (MEG)

The figure 15 represents the relationship between Frequency (in GHz) and Mean Effective Gain (MEG) (in dB).

- The MEG starts at around -7 dB at 25 GHz. As the frequency increases, the MEG rises steadily.
- Between 26 GHz and 30 GHz, the MEG values remain relatively flat and stable, peaking around -6 dB in this range. This indicates a consistent and favorable mean effective gain performance.
- After 30 GHz, the MEG starts to decline, approaching -7 dB again as the frequency nears 31 GHz.

The MEG values in the range from 26 GHz to 30 GHz suggest that the system is operating with good gain efficiency in this band. The gain decreases sharply at the edges of the frequency range (near 25 GHz and 31 GHz), indicating less effective performance outside this central frequency range.

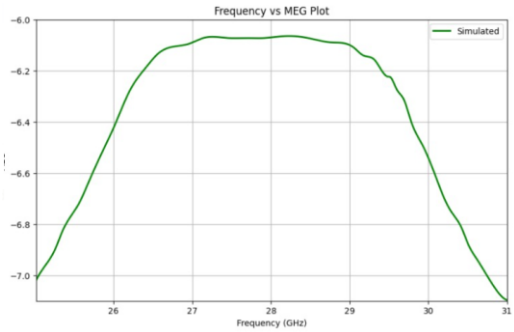

Figure 15: Simulation and measurement of suggested antenna MEG

7.7 Channel Capacity Loss (CCL)

The [figure 16] shows the relationship between Frequency (in GHz) and CCL (in bits/s/Hz).

- At 25 GHz, the CCL is at its highest value of approximately 0.25 bits/s/Hz. As the frequency increases, the CCL decreases steadily.
- The CCL reaches its minimum value of around 0 bits/s/Hz between 27 GHz and 28 GHz, indicating minimal channel capacity loss in this range.
- Beyond 28 GHz, the CCL starts to rise again, reaching around 0.25 bits/s/Hz at 31 GHz, similar to the values observed at the lower end of the frequency spectrum.

The U-shaped curve shows that the system experiences the least CCL (around 0 bits/s/Hz) in the frequency range of 27 GHz to 28 GHz, which is ideal for communication. Outside of this range, the channel capacity loss increases, reaching higher values at both lower and higher frequencies (around 25 GHz and 31 GHz).

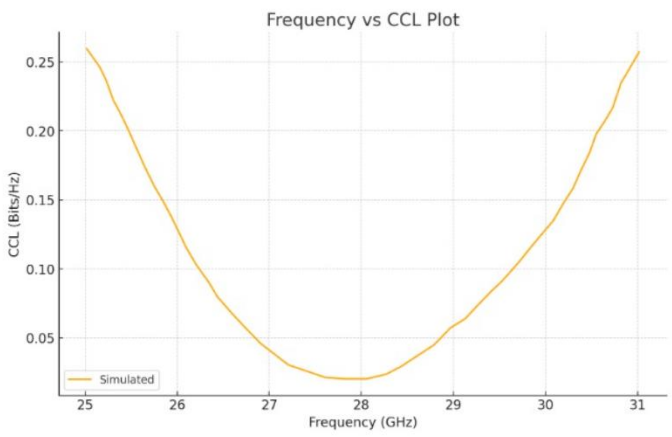

Figure 16: Simulation and measurement of suggested antenna CCL

Journal of Information Systems Engineering and Management
2025, 10(53s)
e-ISSN: 2468-4376
https://www.jisem-journal.com/

Research Article

7.8 Correlation of the Current MIMO Antenna System with Cutting-Edge Developments

The suggested MIMO antenna is compared to existing previous work in [Table 3]. It is clear that the recommended antenna provides a smaller size in comparison to the majority of the published studies. The high ECC and CLL values are a drawback, even if their dimensions are less than the given work [Table 4]. Hence, the suggested work outperformed the remainder because to its small size, wide bandwidth, high gain, and low ECC, CLL, and MEG values.

Table 3: Analyzing the current antenna design in relation to the most recent novel study

Work	Dimensions (mm*mm*mm)	Bandwidth (GHz)	Maximum Gain (dBi)	Radiation Efficiency (%)
Farahat and Hussein (2022)	7.5*8.8*0.25	1.2	6.62	80
Farahat and Hussein (2020)	21.6*20*0.25	3.42	9	98
Alnemr, et al. (2021)	20.4*26.4*0.5	0.7	7.03	86
Chaudhary and Kansal (2023)	10*10*0.254	0.5	7.4	77
Hussain, et al. (2022)	10*10	3.52	7.1	90
Our	$51mm \times 51mm \times 0.9mm^3$	1.5	7.8	94

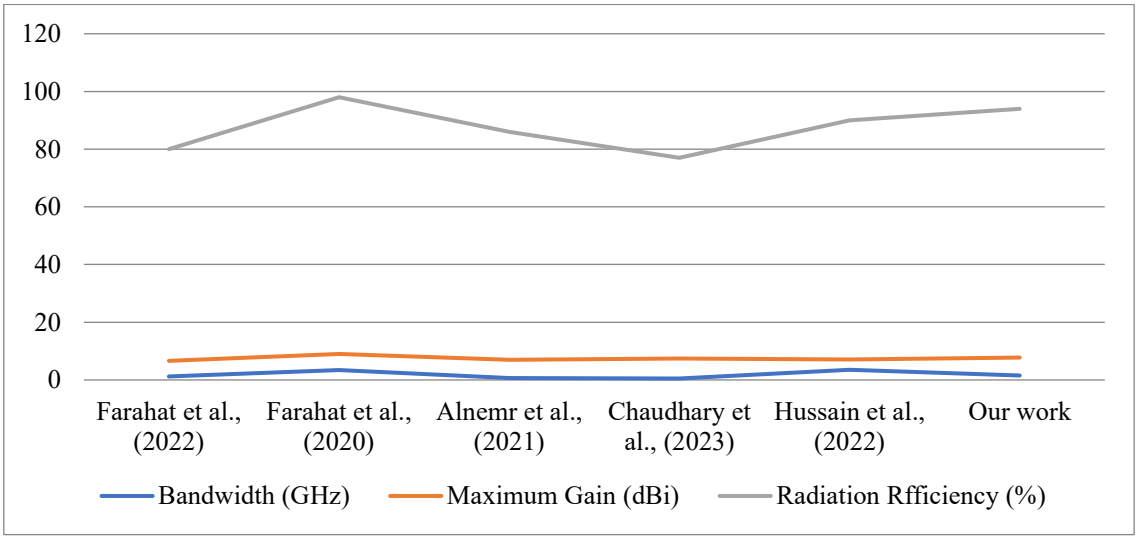

Figure17: Comparing the current antenna design to the SOTA research

Table 4: Comparison of planned work with other works

Ref.	Dimension	No. of ports	Bandwidth	Gain	ECC	CLL
Khalid, et al. (2020)	30*35	4	4.1	8.3	0.5	0.4

Research Article

Khalid, et al. (2019)	28*30	4	3	6.2	0.05	0.2
Tu, et al. (2017)	11*31	4	5	10	0.04	0.5
Arabi, et al. (2020)	60*100	2	1.7	9.8	-	0.002
Hussain, et al. (2022)	30*30	4	4	7.1	0.0005	0.15
Our	$51mm \times 51mm \times 0.9mm^3$	4	1.5	7.8	0.00046	0.25

8. CONCLUSION

The primary objective of this study is to develop and evaluate a unique MIMO antenna that is specifically designed for the mm wave band operating at 28 GHz. This band is an important frequency for 5G applications. MIMO systems operating at mm Wave frequencies provide potential solutions by delivering greater capacity and spectral efficiency. This addresses the increasing need for accelerated data speeds and enhanced communication efficacy. The created antenna aims to optimize performance regarding gain, bandwidth, and radiation efficiency. It aims to address challenges inherent to millimeter wave frequencies, including significant route loss and limited coverage. The discrepancy among the ECC and the DG is less than 9.59, whereas the difference with the CCL is less than 0.25. Throughout the manufacturing manipulate, the conventional single-element antennas and the MIMO are experimentally evaluated, demonstrating effective matching of impedance across all the bands of frequency. These findings align with the computer simulation results. The antenna has an effective gain of 7.8 dBi at a frequency of 28. The proposed antenna has an average transmission effectiveness of 94% across all different frequency bands. Furthermore, the coupling coefficients of the MIMO antenna systems were experimentally evaluated, revealing minimal coupling, hence indicating a viable MIMO system for upcoming mm-wave communication.

REFERENCES

[1] Aboualalaa, M., & Mansour, I. (2023). Dual-band end-fire four-element MIMO antenna array using split-ring structure for mm-wave 5G applications. *IEEE Access*, *11*, 57383–57390. doi:10.1109/ACCESS.2023.3282706.

[2] Ahmad, A., Choi, D.-Y., & Ullah, S. (2022). A compact two elements MIMO antenna for 5G communication. *Scientific Reports*, *12*(1), 3608. doi:10.1038/s41598-022-07579-5.

[3] Alnemr, F., Ahmed, M. F., & Shaalan, A. A. (2021). A compact 28/38 GHz MIMO circularly polarized antenna for 5 G applications. *Journal of Infrared, Millimeter, and Terahertz Waves*, *42*(3), 338–355. doi:10.1007/s10762-021-00770-1.

[4] Arabi, Omer, Chan Hwang See, Arabi, O., See, C. H., Ullah, A., Ali, N., Liu, B., Abd-Alhameed, R. et al. (2020). Compact wideband MIMO diversity antenna for mobile applications using multi-layered structure. *Electronics*, *9*(8), 1307. doi:10.3390/electronics9081307.

[5] Chae, S. H., Oh, S.-K., & Park, S.-O. (2007). Analysis of mutual coupling, correlations, and TARC in WiBro MIMO array antenna. *IEEE Antennas and Wireless Propagation Letters*, *6*, 122–125. doi:10.1109/LAWP.2007.893109.

[6] Chaudhary, S., & Kansal, A. (2023). Compact high gain 28, 38 GHz antenna for 5G communication. *International Journal of Electronics*, *110*(6), 1028–1048. doi:10.1080/00207217.2022.2068201.

[7] Costanzo, S., Venneri, F., Di Massa, G., Borgia, A., Costanzo, A., & Raffo, A. (2016). Fractal reflectarray antennas: state of art and new opportunities. *International Journal of Antennas and Propagation*, *2016*(1), 1–17. doi:10.1155/2016/7165143.

[8] Elabd, R. H., & Al-Gburi, A. J. A. (2024). Super-compact 28/38 GHz 4-port MIMO antenna using metamaterial-inspired EBG structure with SAR analysis for 5G cellular devices. *Journal of Infrared, Millimeter, and Terahertz Waves*, *45*(1–2), 35–65. doi:10.1007/s10762-023-00959-6.

[9] Farahat, A. E., & Hussein, K. F. A. (2020). 28/38 GHz dual-band Yagi-Uda antenna with corrugated radiator and enhanced reflectors for 5G MIMO antenna systems. *Progress in Electromagnetics Research C*, *101*, 159–172. doi:10.2528/PIERC20022603.

[10] Farahat, A. E., & Hussein, K. F. A. (2022). Dual-band (28/38 GHz) wideband MIMO antenna for 5G mobile applications. *IEEE Access*, *10*, 32213–32223. doi:10.1109/ACCESS.2022.3160724.

[11] Garg, P., & Jain, P. (2020). Isolation improvement of MIMO antenna using a novel flower shaped metamaterial absorber at 5.5 GHz WiMAX band. *IEEE Transactions on Circuits and Systems II*, *67*(4), 675–679. doi:10.1109/TCSII.2019.2925148.

[12] Gupta, A., Kumari, M., Sharma, M., Alsharif, M. H., Uthansakul, P., Uthansakul, M. et al. (2024). 8-port MIMO antenna at 27 GHz for n261 band and exploring for body centric communication. *PLOS One*, *19*(6), Article e0305524. doi:10.1371/journal.pone.0305524.

[13] Hong, W. (2017). Solving the 5G mobile antenna puzzle: assessing future directions for the 5G mobile antenna paradigm shift. *IEEE Microwave Magazine*, *18*(7), 86–102. doi:10.1109/MMM.2017.2740538.

[14] Hussain, M., Mousa Ali, E. M., Jarchavi, S. M. R., Zaidi, A., Najam, A. I., Alotaibi, A. A. et al. (2022). Design and characterization of compact broadband antenna and its MIMO configuration for 28 GHz 5G applications. *Electronics*, *11*(4), 523. doi:10.3390/electronics11040523.

[15] Hussain, N., Jeong, M.-J., Abbas, A., & Kim, N. (2020). Metasurface-based single-layer wideband circularly polarized MIMO antenna for 5G millimeter-wave systems. *IEEE Access*, *8*, 130293–130304. doi:10.1109/ACCESS.2020.3009380.

[16] Hussain, R., Abou-Khousa, M., Iqbal, N., Algarni, A., Alhuwaimel, S. I., Zerguine, A. et al. (2022). A multiband shared aperture MIMO antenna for millimeter-wave and sub-6GHz 5G applications. *Sensors*, *22*(5), 1808. doi:10.3390/s22051808.

[17] Ibrahim, M. S. (2019). Design of low-cost, circularly polarized, and wideband U-slot microstrip patch antenna with parasitic elements for WiGig and WPAN applications. *Applied Computational Electromagnetics Society Journal (ACES)*, 1453–1456.

[18] Khalid, H., Khalid, M., Fatima, A., & Khalid, N.. "2×2 MIMO antenna with defected ground structure for mm-wave 5G applications." (2019). In 13th International Conference on Mathematics, Actuarial Science, Computer Science and Statistics (MACS) (pp. 1–6). New York: IEEE.

[19] Khalid, M., Iffat Naqvi, S. I., Hussain, N., Rahman, M.U., Fawad, S. S. M., Mirjavadi, S. S. et al. (2020). 4-Port MIMO antenna with defected ground structure for 5G millimeter wave applications. *Electronics*, *9*(1), 71. doi:10.3390/electronics9010071.

[20] Khan, M. I., Khan, S., Kiani, S. H., Ojaroudi Parchin, N. O., Mahmood, K., Rafique, U. et al. (2022). A compact mmWave MIMO antenna for future wireless networks. *Electronics*, *11*(15), 2450. doi:10.3390/electronics11152450.

[21] Kiani, S. H., Marey, M., Rafique, U., Shah, S. I. H., Bashir, M. A., Mostafa, H. et al. (2022). A deployable and cost-effective kirigami antenna for Sub-6 GHz MIMO applications. *Micromachines*, *13*(10), 1735. doi:10.3390/mi13101735.

[22] Kiani, S. H., Marey, M., Savci, H. Ş., Mostafa, H., Rafique, U., & Khan, M. A. (2022). Dual-band multiple-element MIMO antenna system for next-generation smartphones. *Applied Sciences*, *12*(19), 9694. doi:10.3390/app12199694.

[23] Munir, M. E., Kiani, S. H., Savci, H. S., Marey, M., Khan, J., Mostafa, H. et al. (2023). A four element mm-wave MIMO antenna system with wide-band and high isolation characteristics for 5G applications. *Micromachines*, *14*(4), 776. doi:10.3390/mi14040776.

[24] Munir, M. E., Nasralla, M. M., & Esmail, M. A. (2024). Four port tri-circular ring MIMO antenna with wide-band characteristics for future 5G and mmWave applications. *Heliyon*, *10*(8), Article e28714. doi:10.1016/j.heliyon.2024.e28714.

Research Article

[25] Nasri, N. E. H., El Ghzaoui, M. E. L., Das, S., Islam, T., Ali, W., & Fattah, M. (2024). A novel arc-shaped four-port wideband (21.8–29.1 GHz) MIMO antenna with improved characteristics for 5G NR networks. *International Journal of Communication Systems*, *37*(7), Article e5746. doi:10.1002/dac.5746.

[26] Niu, Z., Zhang, H., Chen, Q., & Zhong, T. (2019). Isolation enhancement for 1×3 Closely Spaced E-Plane Patch Antenna Array Using Defect Ground Structure and Metal-Vias. *IEEE Access*, *7*, 119375–119383. doi:10.1109/ACCESS.2019.2937385.

[27] Patre, S. R., & Singh, S. P. (2016). Broadband multiple-input–multiple-output antenna using castor leaf-shaped quasi-self-complementary elements. *IET Microwaves, Antennas and Propagation*, *10*(15), 1673–1681. doi:10.1049/iet-map.2016.0058.

[28] Raj, T., Mishra, R., Kumar, P., & Kapoor, A. (2023). Advances in MIMO antenna design for 5G: A comprehensive review. *Sensors*, *23*(14), 6329. doi:10.3390/s23146329.

[29] Raj, U., Kumar Sharma, M. K., Singh, V., Javed, S., & Sharma, A. (2021). Easily extendable four port MIMO antenna with improved isolation and wide bandwidth for THz applications. *Optik*, *247*, Article 167910. doi:10.1016/j.ijleo.2021.167910.

[30] Sharawi, M. S. (2013). Printed multi-band MIMO antenna systems and their performance metrics [wireless corner]. *IEEE Antennas and Propagation Magazine*, *55*(5), 218–232. doi:10.1109/MAP.2013.6735522.

[31] Sridevi, S., & Mahendran, K. (2017). Design of millimeter-wave microstrip patch antenna for MIMO communication. *International Research Journal of Engineering and Technology*, *4*(10), 1513–1518.

[32] Tiwari, R. N., Sharma, D., Singh, P., & Kumar, P. (2024). A flexible dual-band 4× 4 MIMO antenna for 5G mm-wave 28/38 GHz wearable applications. *Scientific Reports*, *14*(1), Article 14324. doi:10.1038/s41598-024-65023-2.

[33] Tiwari, R. N., Singh, P., Kumar, P., & Kanaujia, B. K. (2022). High isolation 4-port UWB MIMO antenna with novel decoupling structure for high speed and 5G communication. In International Conference on Electromagnetics in Advanced Applications (ICEAA) (pp. 336–339). New York: IEEE. doi:10.1109/ICEAA49419.2022.9900029.

[34] Tsao, Y.-F., Desai, A., & Hsu, H.-T. (2022). Dual-band and dual-polarization CPW fed MIMO antenna for fifth-generation mobile communications technology at 28 and 38 GHz. *IEEE Access*, *10*, 46853–46863. doi:10.1109/ACCESS.2022.3171248.

[35] Tu, D. T. T., Thang, N. G., Ngoc, N. T., Phuong, N. T. B., & Van Yem, V. (2017). 28/38 GHz dual-band MIMO antenna with low mutual coupling using novel round patch EBG cell for 5G applications. In International Conference on Advanced Technologies for Communications (ATC) (pp. 64–69). New York: IEEE.

[36] Zahra, H., Awan, W. A., Ali, W. A. E., Hussain, N., Abbas, S. M., & Mukhopadhyay, S. (2021). A 28 GHz broadband helical inspired end-fire antenna and its MIMO configuration for 5G pattern diversity applications. *Electronics*, *10*(4), 405. doi:10.3390/electronics10040405.